ISSN 1674-1056
http://cpb.iphy.ac.cn
http://iopscience.iop.org/cpb
中国物理 B
Chinese Physics
中国物理 Chinese Physics B

Potentials of classical force fields for interactions between Na^+ and carbon nanotubes

De-Yuan Li(李德远), Guo-Sheng Shi(石国升), Feng Hong(洪峰), Hai-Ping Fang(方海平)
Citation: Chin. Phys. B . 2018, 27(9): 098801. **doi:** 10.1088/1674-1056/27/9/098801

Journal homepage: http://cpb.iphy.ac.cn; http://iopscience.iop.org/cpb

What follows is a list of articles you may be interested in

Dependence of the solar cell performance on nanocarbon/Si heterojunctions

Shiqi Xiao(肖仕奇), Qingxia Fan(范庆霞), Xiaogang Xia(夏晓刚), Zhuojian Xiao(肖卓建), Huiliang Chen(陈辉亮), Wei Xi(席薇), Penghui Chen(陈鹏辉), Junjie Li(李俊杰), Yanchun Wang(王艳春), Huaping Liu(刘华平), Weiya Zhou(周维亚)
Chin. Phys. B . 2018, 27(7): 078801. **doi:** 10.1088/1674-1056/27/7/078801

Detection of invisible phonon modes in individual defect-free carbon nanotubes by gradient-field Raman scattering

Feng Yang(杨丰), Yinglu Ji(纪英露), Xiao Zhang(张霄), Qingxia Fan(范庆霞), Nan Zhang(张楠), Xiaogang Gu(谷孝刚), Zhuojian Xiao(肖卓建), Qiang Zhang(张强), Yanchun Wang(王艳春), Xiaochun Wu(吴晓春), Junjie Li(李俊杰), Weiya Zhou(周维亚)
Chin. Phys. B . 2017, 26(7): 078801. **doi:** 10.1088/1674-1056/26/7/078801

Design and optimization of carbon nanotube/polymer actuator by using finite element analysis

Wei Zhang(张薇), Luzhuo Chen(陈鲁倬), Jianmin Zhang(张健敏), Zhigao Huang(黄志高)
Chin. Phys. B . 2017, 26(4): 048801. **doi:** 10.1088/1674-1056/26/4/048801

Highly conductive and transparent carbon nanotube-based electrodes for ultrathin and stretchable organic solar cells

Qingxia Fan(范庆霞), Qiang Zhang(张强), Wenbin Zhou(周文斌), Feng Yang(杨丰), Nan Zhang(张楠), Shiqi Xiao(肖仕奇), Xiaogang Gu(谷孝刚), Zhuojian Xiao(肖卓建), Huiliang Chen(陈辉亮), Yanchun Wang(王艳春), Huaping Liu(刘华平), Weiya Zhou(周维亚)
Chin. Phys. B . 2017, 26(2): 028801. **doi:** 10.1088/1674-1056/26/2/028801

Performance improvement of continuous carbon nanotube fibers by acid treatment

Qiang Zhang(张强), Kewei Li(李克伟), Qingxia Fan(范庆霞), Xiaogang Xia(夏晓刚), Nan Zhang(张楠), Zhuojian Xiao(肖卓建), Wenbin Zhou(周文斌), Feng Yang(杨丰), Yanchun Wang(王艳春), Huaping Liu(刘华平), Weiya Zhou(周维亚)
Chin. Phys. B . 2017, 26(2): 028802. **doi:** 10.1088/1674-1056/26/2/028802

Potentials of classical force fields for interactions between Na^+ and carbon nanotubes*

De-Yuan Li(李德远)[1,2], Guo-Sheng Shi(石国升)[1,2,†], Feng Hong(洪峰)[1,‡], and Hai-Ping Fang(方海平)[1,2]

[1] *Department of Physics and Shanghai Applied Radiation Institute, Shanghai University, Shanghai* 200444, *China*

[2] *Division of Interfacial Water and Key Laboratory of Interfacial Physics and Technology, Shanghai Institute of Applied Physics, Chinese Academy of Sciences, Shanghai* 201800, *China*

(Received 11 May 2018; revised manuscript received 7 June 2018; published online 28 August 2018)

Carbon nanotubes (CNTs) have long been expected to be excellent nanochannels for use in desalination membranes and other bio-inspired human-made channels owing to their experimentally confirmed ultrafast water flow and theoretically predicted ion rejection. The correct classical force field potential for the interactions between cations and CNTs plays a crucial role in understanding the transport behaviors of ions near and inside the CNT, which is key to these expectations. Here, using density functional theory calculations, we provide classical force field potentials for the interactions of Na^+/hydrated Na^+ with (7,7), (8,8), (9,9), and (10,10)-type CNTs. These potentials can be directly used in current popular classical software such as nanoscale molecular dynamics (NAMD) by employing the tclBC interface. By incorporating the potential of hydrated cation-π interactions to classical all-atom force fields, we show that the ions will move inside the CNT and accumulate, which will block the water flow in wide CNTs. This blockage of water flow in wide CNTs is consistent with recent experimental observations. These results will be helpful for the understanding and design of desalination membranes, new types of nanofluidic channels, nanosensors, and nanoreactors based on CNT platforms.

Keywords: carbon nanotube, density functional theory, force field, molecular dynamics simulation

PACS: 88.30.rh, 31.15.E, 87.10.Tf **DOI:** 10.1088/1674-1056/27/9/098801

1. Introduction

A nanotube that enables fast water flow while rejecting ions is of great importance in water desalination and purification,[1–6] nanofluidics manipulation,[7–12] ion detection,[13] drug delivery,[14,15] nanodevice fabrication,[16–21] and biomimetic membrane pore design.[22,23] It has been found that carbon nanotubes (CNTs) have an extra high water flow rate from theoretical simulations[24–28] and experimental observations.[29,30] In 2001, Hummer *et al.*[24] theoretically predicted the potential effectiveness of water flow in nanotubes using a molecular dynamics (MD) simulation, and in 2006, Holt *et al.*[30] experimentally demonstrated that the water permeability of CNT-based membranes is several orders of magnitude higher than that expected from conventional hydrodynamic theories. Using classical MD simulations based on traditional force fields, it has been theoretically shown that narrower CNTs, with diameters smaller than the size of hydrated ions, would reject the passage of ions while still maintaining ultrahigh permeability for the water flow; an example is a (6,6)-type CNT with a diameter of ~ 0.5 nm.[25,31]

With the benefit of this unique property of fast water flow combined with ion rejection, narrower CNTs have been expected to be good candidates for water desalination and purification channels for a decade.[31,32] However, to date, there has been insufficient experimental demonstration of salt rejection adequate for desalination using pristine CNTs.[2] Moreover, for wide CNTs (inner diameter above 1 nm), several experiments[33–35] have shown that there is only very, and even negligibly, small water flow and ion permeation across the CNTs without the addition of pressure or electric field above a threshold. In contrast, results based on popular classical MD simulations showed that there should be fast water permeation across wider tubes.[31] One of the main reasons is the lack of a correct classical force field potential for the interactions between cations and different CNTs, which results in an incomplete understanding of the transport behaviors of ions near and inside the CNT.

Recently, by incorporating the cation-π interaction potential[3] to classical all-atom force fields, we found that cations block water flow through narrow (6,6)-type CNTs due to interactions between cations and aromatic rings in CNTs. In wide CNTs (8,8), these interactions trap the cations in the interior of the CNT, inducing unexpected open or closed state switching of ion transfer under a strong electric field, which is consistent with experiments. More appropriate classical force field potentials for the interactions between cations and other CNTs are expected to enable better understanding of the solution transport behaviors of ions near and inside CNTs. Here,

*Project supported by the National Science Fund for Outstanding Young Scholars of China (Grant No. 11722548) and the National Natural Science Foundation of China (Grant Nos. 11574339 and 11404361).

†Corresponding author. E-mail: gsshi@shu.edu.cn

‡Corresponding author. E-mail: fenghong@shu.edu.cn

© 2018 Chinese Physical Society and IOP Publishing Ltd

we provide classical force field potentials for the interactions of Na^+/hydrated Na^+ with (7,7), (8,8), (9,9), and (10,10)-type CNTs using density functional theory (DFT) calculations, which can be directly used in current popular classical software such as nanoscale molecular dynamics (NAMD) by employing the tclBC interface. For an (8,8)-type CNT, compared to our previous potential,[3] we provide a more accurate classical force field potential for the interactions of Na^+/hydrated Na^+ adsorbing inside an (8,8)-type CNT. This will facilitate further CNT-based research and applications.

2. Methods

We built four armchair CNT clusters with different curvatures: (7,7), (8,8), (9,9), and (10,10), corresponding to molecular formulas $C_{168}H_{28}$, $C_{192}H_{32}$, $C_{216}H_{36}$, and $C_{240}H_{40}$, respectively. All their entrances were passivated by H atoms. The lengths of the (7,7), (8,8), (9,9), and (10,10)-type CNTs (along the tube axis, defined as the Z axis) were approximately 15.4 Å. They contained five aromatic rings, and both ends had H atoms attached. Their diameters were 9.6 Å, 10.9 Å, 12.3 Å, and 13.6 Å after DFT optimization.

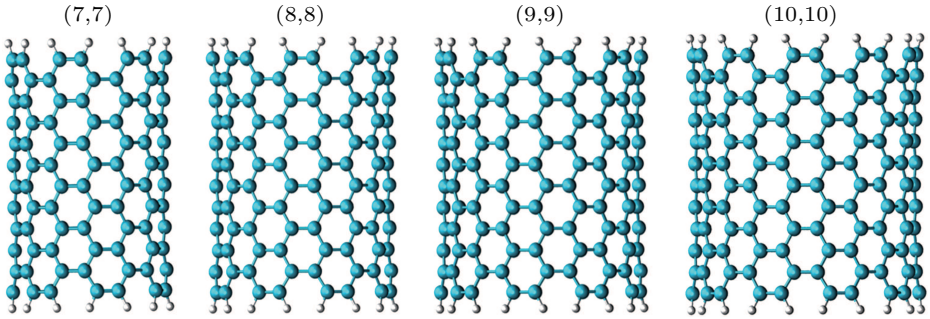


Fig. 1. (color online) The side views of carbon nanotubes (CNTs) with different curvatures: (7,7), (8,8), (9,9), and (10,10).

The original configurations of the (7,7), (8,8), (9,9), and (10,10)-type CNTs were derived from the visual package visual molecular dynamics (VMD).[36] First, the atoms of the four CNT models were freely optimized to obtain the most stable CNT structures, shown in Fig. 1. These stable CNTs were further used to optimize the most stable geometric structures for Na^+/hydrated Na^+ ions in the center of the CNT and at the entrance of these CNTs. We defined the corresponding adsorption energies of Na^+ and hydrated Na^+ in the center of CNTs as ΔE_g and ΔE_l, and those at the entrance of the CNTs as $\Delta E'_g$ and $\Delta E'_l$, respectively. Next, we scanned the adsorption energy curves from the center to the outside of the CNTs along the Z axis with steps of 0.6 Å using the Gaussian 09 program.[37] In hydrated systems, an Na^+ ion combines with six water molecules.[3,38] All calculations on the optimized geometric structures were performed with the B3LYP/6-31G(d) model, which was widely employed in studies of the interactions of carbon-based materials with ions.[3,39–46]

3. Results and discussion

3.1. Adsorption of Na^+ in the center and at the entrance of (7,7), (8,8), (9,9), and (10,10)-type CNTs

In our previous work,[3] we provided the classical force field potentials for the interactions of Na^+/hydrated Na^+ with (6,6) and (8,8)-type CNTs by simply scanning the interaction energies along the central axis of the tubes using DFT calculations. This method is relatively rough for wide tubes such as (8,8)-type CNTs since the most stable cation adsorption sites are not always in the central axis of the tube. In this work, we provide more accurate potentials for Na^+/hydrated Na^+ inside wide tubes. First, we optimized the geometric structures for Na^+ ions in the center (the point along the Z axis defined as the original point, $Z = 0$ Å) and at the entrance ($Z = 7.8$ Å) of (7,7), (8,8), (9,9), and (10,10)-type CNTs. We note that there are three different types of site inside CNTs. We investigated the most stable Na^+ structure in a (7,7)-type CNT in PS1 of the ESI. We obtained results similar to our previous study,[40] which are that the H site is the most stable, the B sites are sub-stable, and the T site is unstable, where the Na^+ ion moves to the H site during geometry optimization. The most stable structures of the system using (7,7)-type CNTs as examples are shown in Figs. 2(a)–2(c), and the other systems are shown in PS2 of the ESI. To study the stability of Na^+ with different CNTs, we calculated the adsorption energies (ΔE_g) of Na^+ ions with CNTs, which are defined as

$$\Delta E_g = E_{Na^+-CNT} - E_{CNT} - E_{Na^+}, \quad (1)$$

where E_{Na^+-CNT}, E_{CNT}, and E_{Na^+} are the total energies of the Na^+ ion with the CNT, the CNT clusters, and the Na^+ ion alone, respectively.

These adsorption energies are shown in Fig. 3. We note that the adsorption energies of Na^+ in the center of the CNTs are over 42 kcal/mol, which is about seven times that of the hydrogen binding energy of two water molecules at the same temperature, indicating that the adsorption of Na^+ in the center of the CNTs is quite stable at room temperature. The adsorption energies will be largely reduced when the Na^+ ion moves from the center of the CNTs to the entrance of these

CNTs. This indicates that Na^+ prefers to be inside these tubes. The adsorption energy of Na^+ in the center of a (9,9)-type CNT is 1.0 kcal/mol, 0.3 kcal/mol, and 0.6 kcal/mol larger than that of Na^+ in the center of (7,7), (8,8), and (10,10)-type CNTs, respectively. Adsorption energy of Na^+ at the entrance of a (7,7)-type CNT is 0.3 kcal/mol, 0.3 kcal/mol, and 1.0 kcal/mol larger than that of Na^+ at the entrance of (8,8), (9,9), and (10,10)-type CNTs, respectively. We have performed a residuary charges analysis to illustrate the physical nature of the cation-π interaction between an Na^+ ion and a single-walled CNT. We find the Hirshfeld charge transfer is consistent with the adsorption energies of Na^+ at the entrances of different CNTs, as shown in PS3 of the ESI.

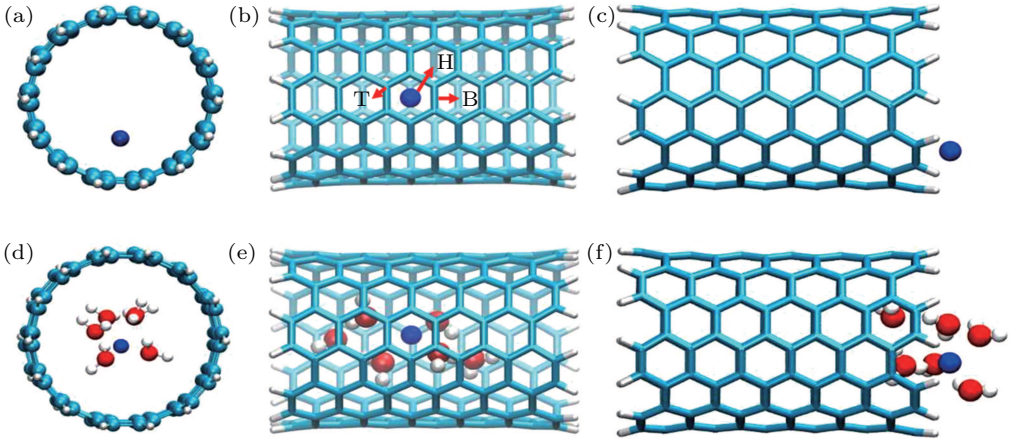


Fig. 2. (color online) (a), (d) Top views and (b), (e) side views of Na^+/hydrated Na^+, respectively, in the most stable geometric structures in the center of a (7,7)-type CNT. (c) and (f) Side views of the most stable geometric structures of the Na^+ and hydrated Na^+, respectively, at the entrance of a (7,7)-type CNT. In panel (b), the different adsorption sites are shown, i.e., above the hollow (H), C–C bond (B), and carbon atom top (T) sites of the hexagonal ring.

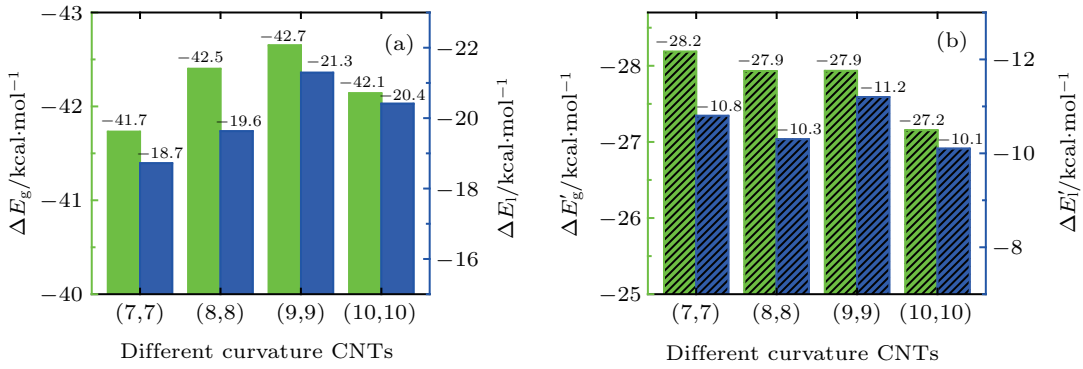


Fig. 3. (color online) Adsorption energies of Na^+ (ΔE_g) and hydrated Na^+ (ΔE_l) in the center (a) and at the entrance (b) of (7,7), (8,8), (9,9), and (10,10)-type CNTs.

3.2. Adsorption of hydrated Na^+ in the center and at the entrance of (7,7), (8,8), (9,9), and (10,10)-type CNTs

Hydrated Na^+ combined with six water molecules adsorbed in (7,7), (8,8), (9,9), and (10,10)-type CNTs was investigated, with the corresponding adsorption sites at $Z = 0$ Å and $Z = 7.8$ Å. When comparing with Na^+ at the H site, B site, and T site, we found the H site is also the most stable for hydrated Na^+ in (7,7)-type CNTs. The geometric structures and the adsorption energies are shown in PS4 of the ESI. We also investigated the different hydrated Na^+ conformers to find the most stable conformer at the H site in PS5 of the ESI. Examples of the most stable structures of the system for (7,7)-type CNTs are shown in Figs. 2(d)–2(e). According to previous work, the adsorption energies (ΔE_l) of the hydrated Na^+ with the CNT were calculated as follows:[3]

$$\Delta E_l = \Delta E_{CNT-Na^+\cdot(H_2O)_6} - \Delta E_{CNT-(H_2O)_6}, \quad (2)$$

where $\Delta E_{CNT-Na^+\cdot(H_2O)_6}$ is the total interaction energy of the hydrated Na^+ with the CNT, and $\Delta E_{CNT-(H_2O)_6}$ is the interaction energy of the water cluster with the CNT.

$$\begin{aligned}\Delta E_l &= (E_{CNT-Na^+\cdot(H_2O)_6} - E_{Na^+\cdot(H_2O)_6} - E_{CNT}) \\ &\quad - (E_{CNT-(H_2O)_6} - E_{CNT} - E_{(H_2O)_6}) \\ &= E_{CNT-Na^+\cdot(H_2O)_6} - E_{CNT-(H_2O)_6}\end{aligned}$$

$$
\begin{aligned}
&-E_{\mathrm{Na^+\cdot(H_2O)_6}}+E_{\mathrm{(H_2O)_6}}\\
&=(E_{\mathrm{CNT-Na^+\cdot(H_2O)_6}}-E_{\mathrm{CNT-(H_2O)_6}})\\
&-(E_{\mathrm{Na^+\cdot(H_2O)_6}}-E_{\mathrm{(H_2O)_6}}),
\end{aligned}
\tag{3}
$$

where $E_{\mathrm{CNT-Na^+\cdot(H_2O)_6}}$ and $E_{\mathrm{Na^+\cdot(H_2O)_6}}$ are the optimized energy of hydrated Na^+ with CNT and the total energy of six waters with Na^+, while $E_{\mathrm{CNT-(H_2O)_6}}$ and $E_{\mathrm{(H_2O)_6}}$ are the energies of corresponding geometries taken from the optimized structure of $\mathrm{CNT-Na^+\cdot(H_2O)_6}$.

From Fig. 3, we find the adsorption energies of hydrated Na^+ at $Z=0$ Å and $Z=7.8$ Å are around 20 kcal/mol and 10 kcal/mol, respectively, which indicates that hydrated Na^+ in the center of a CNT is more stable than at the entrance. Even though the adsorption energies of hydrated Na^+ are about half of the energies of Na^+ with CNTs, they still are over three times the hydrogen binding energy in the center of CNTs. In addition, the adsorption energies of hydrated Na^+ have similar change tendencies to Na^+.

3.3. The classical force field potentials for the interactions between Na^+/hydrated Na^+ and (7,7), (8,8), (9,9), and (10,10)-type CNTs

Moving the Na^+ ion along the inner wall with fixed Z coordinate while freely varying the X and Y coordinates can reveal the most stable points of adsorption energies between Na^+ and CNTs with Z ranging from $Z=0$ Å to $Z=\pm10.2$ Å. Fitting these points as curves can reveal the classical force field potential for the interactions between Na^+ and CNTs. The curve fits, shown in Fig. 4(a), exhibit two distinct shapes inside the CNT (-5 Å $<Z<5$ Å) and outside the CNT ($Z<-5$ Å or $Z>5$ Å). Therefore, the potential energy curve is treated as a piecewise function with a symmetric cosine function inside the CNT and an arctan function outside the CNT

$$
E_{\mathrm{cation}-\pi}(Z)=\begin{cases}\varepsilon[\beta\cos(\lambda_{\mathrm{in}}\cdot Z)+\lambda], & (-5<Z<5),\\ \alpha\varepsilon\{\arctan[\lambda_{\mathrm{out}}(Z-Z_{\mathrm{m}})]+\arctan[\lambda_{\mathrm{out}}(-Z-Z_{\mathrm{m}})]\}, & (Z<-5\ \text{ or }\ Z>5).\end{cases}
\tag{4}
$$

In Eq. (4), Z is the distance between Na^+ and the center (origin point) of the CNT along the tube's axis, ε is the depth of the potential well, which is derived from the adsorption energies of Na^+ in center ($Z=0$ Å) of CNTs calculated by DFT, and the parameters α, β, and λ are the nondimensional fit coefficients adjusting the potential curve for the corresponding adsorption energies. λ_{out}, λ_{in}, and Z_{m} are parameters corresponding to the characteristics of the CNTs.

The seven parameters of the classical force field potential curves for the interactions between Na^+ and (7,7), (8,8), (9,9), and (10,10)-type CNTs are shown in Table 1. According to these parameters, we can obtain the classical force field potential energy curves, as shown in Fig. 4. For hydrated Na^+, the adsorption energies and curve fits are shown in PS6 of the ESI. We find that the function is consistent with Eq. (3) for Na^+, though the depth of the potential well is less than that of Na^+. From Table 1, we can see that the parameter λ_{out} increases from 0.7 $Å^{-1}$ to 2.6 $Å^{-1}$, which means the steepness becomes sharp at the entrance from (7,7) to (10,10) CNT. For interactions between hydrated Na^+ and CNTs, the parameter ε is 18.7 kcal/mol, 19.6 kcal/mol, 21.3 kcal/mol, and 20.4 kcal/mol for (7,7), (8,8), (9,9), and (10,10)-type CNTs, respectively, and the other six parameters of the potential curves of classical force fields remain unchanged.

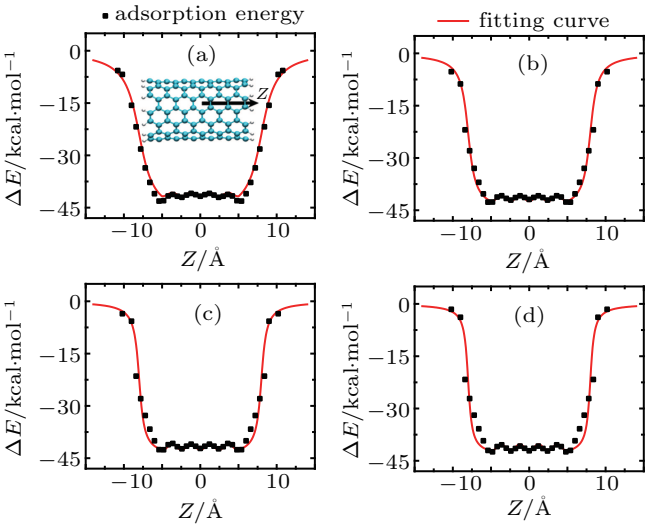


Fig. 4. (color online) (a)–(d) Adsorption energies and curve fits for Na^+ with (7,7), (8,8), (9,9), and (10,10)-type CNTs, respectively.

Table 1. Seven parameters from fitting the potential energy curves of Na^+ ion in CNT systems of different curvatures.

CNT	α	β	λ	ε/kcal·mol^{-1}	λ_{in}/Å^{-1}	λ_{out}/Å^{-1}	Z_{m}/Å
(7,7)	–0.387	0.012	0.988	–41.73	2.56	0.7	8.0
(8,8)	–0.350	0.017	0.983	–42.50	2.56	1.4	8.0
(9,9)	–0.340	0.020	0.980	–42.65	2.56	2.0	8.0
(10,10)	–0.335	0.022	0.978	–42.14	2.56	2.6	8.0

4. Classical simulations adding the cation-π interaction

We use a (9,9)-type CNT as an example. By incorporating the cation-π interaction potential in a classical all-atom force field using the tclBC code (the details of the tclBC code for (7,7), (8,8), (9,9), and (10,10)-type CNTs are shown in PS7 of the ESI), we perform a simulation using a filter membrane containing four (9,9)-type CNTs, as shown in Fig. 5. The filter membrane separates the NaCl aqueous solution from the pure water. There are 60 pairs of NaCl ions along with 3464 water molecules on the left side, and 3513 water molecules on the right side. To obtain water flux, a constant pressure of 20 MPa between the two entrances is applied on the impermeable wall from the NaCl aqueous solution to the pure water side. Additional parameters for classical MD are shown in PS8 of ESI.

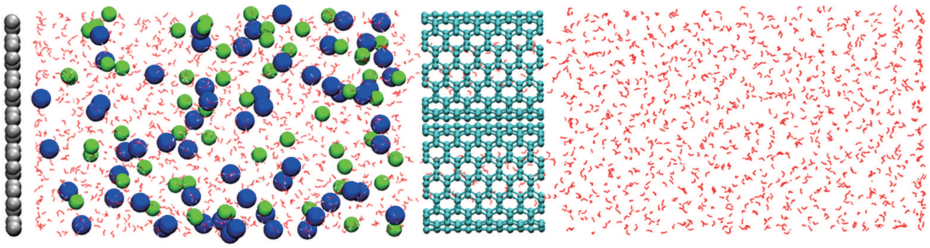


Fig. 5. (color online) Initial carbon nanotube (CNT) filter membrane system containing four (9,9)-type CNTs segregating the NaCl solution and pure water.

Figure 6(a) shows that the ions will move inside the CNT and accumulate. This will block the water flow in wide CNTs (see Fig. 6(c)), which is consistent with recent experimental observation.[34,35] For comparison, we also performed the MD simulation without the cation-π interactions. From Figs. 6(b) and 6(c), we can see that the Na^+ ions are still dispersed in the solution after 10 ns.

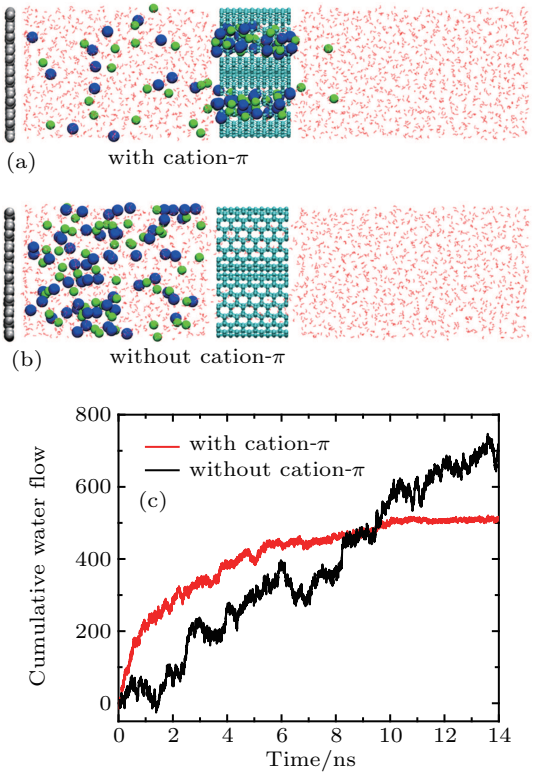


Fig. 6. (color online) (a) Na^+ ions move into the filter membrane consisting of four (9,9)-type CNTs and blocked the water flow at 10 ns with the cation-π interactions. (b) Na^+ ions are still dispersed in the solution without the cation-π interactions at 10 ns. (c) Cumulative water flow with time through the CNT membrane with (red) and without (black) cation-π interactions.

5. Conclusions

We investigated the adsorption energies of Na^+/hydrated Na^+ with (7,7), (8,8), (9,9), and (10,10)-type CNTs in the center and at the entrance using DFT calculations. The results show the interaction between Na^+ with CNTs is quite strong, over 42 kcal/mol in the center and over 27 kcal/mol at the entrance of the CNTs. Although the adsorption energies of hydrated Na^+ with these CNTs are reduced to about half that of Na^+, they remain approximately three times stronger than the hydrogen binding energy in two water molecules at the same temperature.

By scanning the adsorption energies from the inside to the outside of these CNTs and by utilizing the cosine function in conjunction with paired arctan functions, we found the potential curve can be described well by fitting Eq. (3) as a complement to the classical force fields. Based on the potential curves, along with the adsorption energy sharply receding at the entrances of these CNTs, we also found the adsorption energies at the entrance of these CNTs decrease quickly from (7,7) to (10,10)-type CNT.

By incorporating the hydrated cation-π interaction potential obtained here to classical all-atom force fields, we showed that the ions will move inside the CNT and accumulate there. This will block water flow through wide CNTs, which is consistent with recent experimental observations. Our results will help in water desalination and purification, nanofluidic manipulation applications, and other aspects based on the CNT platform.

Acknowledgements

We are grateful to Drs. Jian Liu, Liang Chen, Jinrong Yang, and Yizhou Yang for their helpful discussions. We also thank the support from the Deepcomp 7000 and ScGrid of the

Supercomputing Center, Computer Network Information Center of the Chinese Academy of Sciences, and the Shanghai Supercomputer Center of China.

References

[1] Shannon M A, Bohn P W, Elimelech M, Georgiadis J G, Mariñas B J and Mayes A M 2008 *Nature* **452** 301
[2] Elimelech M and Phillip W A 2011 *Science* **333** 712
[3] Liu J, Shi G S, Guo P, Yang J R and Fang H P 2015 *Phys. Rev. Lett.* **115** 164502
[4] Whitby M and Quirke N 2007 *Nat. Nanotechnol.* **2** 87
[5] Liu J, Shi G S and Fang H P 2017 *Nanotechnology* **28** 084004
[6] Moradi F, Ganji M D and Sarrafi Y 2017 *Phys. Chem. Chem. Phys.* **19** 8388
[7] Wan R Z, Li J Y, Lu H J and Fang H P 2005 *J. Am. Chem. Soc.* **127** 7166
[8] Li J Y, Gong X J, Lu H J, Li D, Fang H P and Zhou R H 2007 *Proc. Natl. Acad. Sci. USA* **104** 3687
[9] Vuković L, Vokac E and Král P 2014 *J. Phys. Chem. Lett.* **5** 2131
[10] Bocquet L and Charlaix E 2010 *Chem. Soc. Rev.* **39** 1073
[11] Su J Y, Zhao Y Z, Fang C, Ahmed S B and Shi Y 2017 *Phys. Chem. Chem. Phys.* **19** 22406
[12] Qin X C, Yuan Q Z, Zhao Y P, Xie S B and Liu Z F 2011 *Nano Lett.* **11** 2173
[13] Howorka S and Siwy Z 2009 *Chem. Soc. Rev.* **38** 2360
[14] Bianco A, Kostarelos K and Prato M 2005 *Curr. Opin. Chem. Biol.* **9** 674
[15] Zang J L, Yuan Q Z, Wang F C and Zhao Y P 2009 *Comput. Mater. Sci.* **46** 621
[16] Hilder T A and Hill J M 2009 *Small* **5** 300
[17] Tasis D, Tagmatarchis N, Bianco A and Prato M 2006 *Chem. Rev.* **106** 1105
[18] Meng S, Wang W L, Maragakis P and Kaxiras E 2007 *Nano Lett.* **7** 2312
[19] Zhao Y and Truhlar D G 2007 *J. Am. Chem. Soc.* **129** 8440
[20] Yuan Q Z and Zhao Y P 2009 *Biomicrofluidics* **3** 6
[21] Yuan Q Z and Zhao Y P 2009 *J. Am. Chem. Soc.* **131** 6374
[22] Garcia-Fandiño R and Sansom M S P 2012 *Proc. Natl. Acad. Sci. USA* **109** 6939
[23] Yang L H, Gordon V D, Trinkle D R, Schmidt N W, Davis M A, DeVries C, Som A, Cronan J E, Tew G N and Wong G C L 2008 *Proc. Natl. Acad. Sci. USA* **105** 20595
[24] Hummer G, Rasaiah J C and Noworyta J P 2001 *Nature* **414** 188
[25] Kalra A, Garde S and Hummer G 2003 *Proc. Natl. Acad. Sci. USA* **100** 10175
[26] Striolo A 2006 *Nano Lett.* **6** 633
[27] Tu Y S, Xiu P, Wan R Z, Hu J, Zhou R H and Fang H P 2009 *Proc. Natl. Acad. Sci. USA* **106** 18120
[28] Falk K, Sedlmeier F, Joly L, Netz R R and Bocquet L 2010 *Nano Lett.* **10** 4067
[29] Majumder M, Chopra N, Andrews R and Hinds B J 2005 *Nature* **438** 44
[30] Holt J K, Park H G, Wang Y M, Stadermann M, Artyukhin A B, Grigoropoulos C P, Noy A and Bakajin O 2006 *Science* **312** 1034
[31] Corry B 2008 *J. Phys. Chem. B* **112** 1427
[32] Jia Y X, Li H L, Wang M, Wu L Y and Hu Y D 2010 *Sep. Purif. Technol.* **75** 55
[33] Secchi E, Marbach S, Nigues A, Stein D, Siria A and Bocquet L 2016 *Nature* **537** 210
[34] Lee C Y, Choi W, Han J and Strano M S 2010 *Science* **329** 1320
[35] Choi W, Lee C Y, Ham M, Shimizu S and Strano M S 2011 *J. Am. Chem. Soc.* **133** 203
[36] Humphrey W, Dalke A and Schulten K 1996 *J. Mol. Graphics* **14** 33
[37] Frisch G W T M J, Schlegel H B, Scuseria G E, *et al.* 2009 *Gaussian 09* (Revision A. 01) (Wallingford CT: Gaussian Inc)
[38] Shi G S, Ding Y H and Fang H P 2012 *J. Comput. Chem.* **33** 1328
[39] Shi G S, Chen L, Yang Y Z, Li D Y, Qian Z, Liang S S, Yan L, Li L H, Wu M H and Fang H P 2018 *Nat. Chem.* **10** 776
[40] Gao S H, Shi G S and Fang H P 2016 *Nanoscale* **8** 1451
[41] Chen L, Shi G S, Shen J, Peng B, Zhang B W, Wang Y Z, Bian F G, Wang J J, Li D Y, Qian Z, Xu G, Liu G P, Zeng J R, Zhang L J, Yang Y Z, Zhou G Q, Wu M H, Jin W Q, Li J Y and Fang H P 2017 *Nature* **550** 380
[42] Shi G S, Dang Y R, Pan T T, Liu X, Liu H, Li S X, Zhang L J, Zhao H W, Li S P, Han J G, Tai R Z, Zhu Y M, Li J C, Ji Q, Mole R A, Yu D H and Fang H P 2016 *Phys. Rev. Lett.* **117** 238102
[43] Lyu G X, Shi G S, Tang L, Fang H P and Wu M H 2017 *Phys. Chem. Chem. Phys.* **19** 9354
[44] Shi G S, Yang J R, Ding Y H and Fang H P 2014 *ChemPhysChem.* **15** 2588
[45] Yang J R, Shi G S, Tu Y S and Fang H P 2014 *Angew. Chem. Int. Ed.* **53** 10190
[46] Shi G S, Liu J, Wang C L, Song B, Tu Y S, Hu J and Fang H P 2013 *Sci. Rep.* **3** 3436